

Degradation mechanism of Schottky P-GaN gate stack in GaN power devices under neutron irradiation

Cite as: Appl. Phys. Lett. **119**, 133503 (2021); doi: [10.1063/5.0065046](https://doi.org/10.1063/5.0065046)

Submitted: 29 July 2021 · Accepted: 13 September 2021 ·

Published Online: 1 October 2021



View Online



Export Citation



CrossMark

Ruize Sun,^{1,2}  Xinghuan Chen,¹ Chao Liu,^{1,3} Wanjun Chen,^{1,2,a)}  and Bo Zhang¹

AFFILIATIONS

¹State Key Laboratory of Electronic Thin Films and Integrated Devices, University of Electronic Science and Technology of China, Chengdu 610054, China

²Institute of Electronic and Information Engineering of UESTC in Guangdong, Dongguan 523808, China

³Chongqing Institute of Microelectronics Industry Technology of UESTC, Chongqing 401332, China

^{a)}Author to whom correspondence should be addressed: wjchen@uestc.edu.cn

ABSTRACT

In this Letter, the degradation mechanism of Schottky p-type GaN (P-GaN) gate stack in GaN power devices under neutron irradiation is studied. After 1-MeV neutron irradiation at fluences of 6×10^{13} and 1×10^{14} neutron/cm², device threshold voltage V_{TH} is positively shifted and gate leakage current is increased, which indicates the degradation of Schottky P-GaN gate stack. By analyzing the gate current with Frenkel–Poole emission model, barrier height of Schottky P-GaN gate stack is reduced due to the traps induced by neutron irradiation. By employing capacitance–voltage (C–V) and pulse current–voltage (I–V) measurements, we find that the electron and hole traps induced by displacement damages dominate the degradation of gate characteristics after neutron irradiation. Electron traps at E_C – (0.38–0.55) eV and hole traps at E_V + (0.56–0.62) eV with a density of 10^{11} – 10^{12} cm^{−2} eV^{−1} are shown in irradiated devices. Ionizations of V_{Ga} and Ga_i induced by neutron radiation as well as their interaction with dislocations significantly alter the energy band of P-GaN/AlGaIn/GaN heterostructure gate stack. The trapping and de-trapping processes of V_{Ga} -related electron traps lead to positive shifts in V_{TH} . Passivation of dislocations by Ga_i effectively lowers the barrier height for holes and increases the gate leakage current. Measures to improve the quality of P-GaN/AlGaIn/GaN heterostructure or raise the potential barrier height can be taken to make the device more resistant to neutron radiation. This work depicts the physical process and mechanism of degradations in Schottky P-GaN gate stack, which can provide deeper insights into the analysis and field application of GaN power devices under neutron irradiation.

Published under an exclusive license by AIP Publishing. <https://doi.org/10.1063/5.0065046>

GaN-based power semiconductor devices have attracted lots of attention in radiation-hard power electronics for near-space or spaceborne applications, such as trips to Mars.^{1,2} Space radiations including γ -rays, protons, heavy-ions, and neutrons can trigger single event upset and total dose failure in semiconductor devices. The wide energy bandgap of 3.4 eV for GaN leads to higher potential barriers than Si and GaAs, which include ionization energy of deep centers, contact potential, and Schottky barrier. The atomic displacement energy, i.e., the energy required to displace an atom from its lattice position, is 20.5 eV for Ga and 10.8 eV for N in GaN.³ In the case of GaAs and Si, it is 9.8 and 12.9 eV, respectively.^{4,5} Although the higher potential barrier and displacement energy of GaN relative to Si and GaAs facilitate high radiation hardness, GaN power devices are still facing susceptibility to degradation and failure under irradiation. For

extreme-environment applications of nuclear or military electronics, neutron irradiated GaN devices could have displacement damages including disordered crystal lattice structure, which can lead to permanent degradations in device performance.⁶

In addition to the structural point defects, dislocations, and disordered regions in GaN material after neutron irradiation,⁷ degradations of device performance including decreased output capability,⁸ shifted threshold voltage (V_{TH}),⁹ forming or “curing” traps,¹⁰ and increased leakage currents¹¹ in neutron irradiated AlGaIn/GaN high-electron-mobility-transistors (HEMTs) have been extensively reported. Deep electron and hole traps induced by neutron irradiation and their dynamic trapping and de-trapping processes are parts of the determinant causes.¹² Unlike the detailed results are reported for P-GaN material or device after proton irradiation,¹³ there are a few works on

neutron irradiated enhancement-mode GaN power devices with P-GaN cap structure. Recently, degradation of the gate stack in GaN power devices after *in situ* electrical bias during neutron irradiation is reported.¹⁴ However, it lacks discussions on the energy band structure of the P-GaN/AlGaIn/GaN heterostructure with the consideration of the traps induced by neutron irradiation, and no mechanism of degradation is reported. Therefore, there is a lack of research on the degradation of Schottky P-GaN/AlGaIn/GaN heterostructure gate stack in GaN power devices under neutron irradiation. The underlying physical mechanism of the degradation needs to be well elucidated.

In this work, we investigate the degradation mechanism of Schottky P-GaN gate stack in GaN power devices under neutron irradiation at fluences of 6×10^{13} and 1×10^{14} neutron/cm². The positive shifts in V_{TH} and increases of gate leakage current are observed. High-frequency capacitance-voltage (C-V) and pulse-mode current-voltage (pulse I-V) measurements are carried out to identify the density and energy level of electron and hole traps in the gate stack. The Ga vacancies and interstitials created by neutron irradiation can be ionized and lead to shifts of V_{TH} , while their interactions with dislocations alter the barrier height for Frenkel-Poole emission of holes in P-GaN/AlGaIn/GaN heterostructure, which accounts for the variations in gate leakage current. The proposed physical mechanism behind the degradation of P-GaN gate stacks can provide deeper insights into the radiation-harden designs and field applications of GaN power devices in the extreme environment with high fluences of neutron irradiation.

The devices under investigation are eighteen pieces of EPC2015C from Efficient Power Conversion Corporation, which are 40-V/53-A enhancement GaN power devices with the Schottky P-GaN gate structure. The epitaxial structure is estimated from the cross-sectional analysis and includes the ~ 70 -nm P-GaN cap layer, ~ 13 -nm AlGaIn barrier layer, ~ 2 - μ m GaN buffer layer, and ~ 550 - μ m Si substrate. The total gate area is estimated to be 7.8×10^{-3} cm². Twelve devices are irradiated by the Chinese Fast Burst Reactor-II in China Academy of Engineering Physics at fluences of 6×10^{13} and 1×10^{14} neutron/cm² (n/cm²) with an average neutron energy of 1 MeV. The I-V and C-V measurements are performed by the Keysight B1505A power device analyzer.

Figure 1(a) shows the measured transferring characteristic with V_{GS} from -4 to 4 V. Compared with the un-irradiated, devices under neutron irradiation with higher fluences exhibit a higher positive shift of V_{TH} (ΔV_{TH}). In Fig. 1(b), the average V_{TH} of each six GaN devices is raised from 1.13 V of the un-irradiated to 1.23 and 1.42 V of the irradiated at fluences of 6×10^{13} and 1×10^{14} n/cm², respectively. The exponential rise of gate current I_{GS} against V_{GS} in Fig. 1(c) indicates the trap-related current conduction mechanism and can be well fitted by the Frenkel-Poole emission model. The rise of I_{GS} against neutron fluences can be attributed to the lowering of barrier height of gate-metal/P-GaN junction, which indicates the degradation of the gate stack. According to the Frenkel-Poole emission model,¹⁵ the change of barrier height $q\Delta\phi_B$ can be obtained by $\ln(I_0/I_N) \cdot kT$, where I_0 and I_N are the I_{GS} of un-irradiated and irradiated devices, respectively, k is the Boltzmann's constant, and T is the temperature. As holes can transfer from the conductive dislocations in P-GaN/AlGaIn/GaN heterostructure to recombine with electrons from the metal Fermi level, the $q\Delta\phi_B$ values of -0.017 and -0.031 eV after neutron irradiation at the fluences of 6×10^{13} and 1×10^{14} n/cm², respectively, indicate the change of dislocation energy state after neutron irradiation. Displacement damages induced by neutron irradiation can form Ga vacancies (V_{Ga}) and interstitials (Ga_i) dominantly in P-GaN and AlGaIn layers due to lower displacement energy of Ga compared with Mg.^{4,16} The V_{Ga} and Ga_i further lead to the degradation of the P-GaN gate stack including shifted V_{TH} and increased gate leakage current through ionization by themselves and interaction with dislocations.¹⁷

The C-V measurement is performed by biasing the gate electrode with a frequency from 1 kHz to 3 MHz and source/drain electrodes grounded. Figure 2(a) shows the typical C-V curves of GaN devices irradiated at the fluence of 1×10^{14} n/cm² with the frequency of 1 kHz to 3 MHz. The C-V curves of devices including un-irradiated and irradiated at the fluence of 6×10^{13} n/cm² show similar trends, so they are not shown here. In Fig. 2(a), two slopes exist at frequency f of 1 – 50 kHz, but the second downward slope diminishes sharply with the frequency higher than 50 kHz, which is different from the upward second slope of metal-insulator-semiconductor HEMTs. The second slope is contributed by the trapping and de-trapping processes of hole

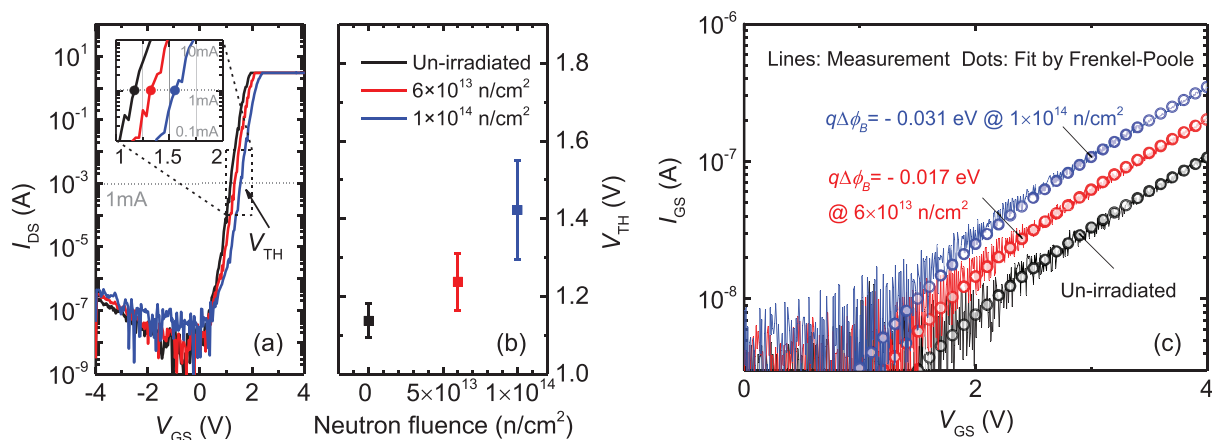


FIG. 1. (a) Measured I_{DS} - V_{GS} curves, (b) V_{TH} vs neutron fluence, and (c) I_{GS} - V_{GS} curves of GaN devices including un-irradiated and irradiated at fluences of 6×10^{13} and 1×10^{14} n/cm², respectively. The inset in (a) is the enlarged view of I_{DS} - V_{GS} curves showing the V_{TH} (solid dots). The open dots in (c) are fitted data using the Frenkel-Poole emission model, and $q\Delta\phi_B$ is the decrease in barrier height.

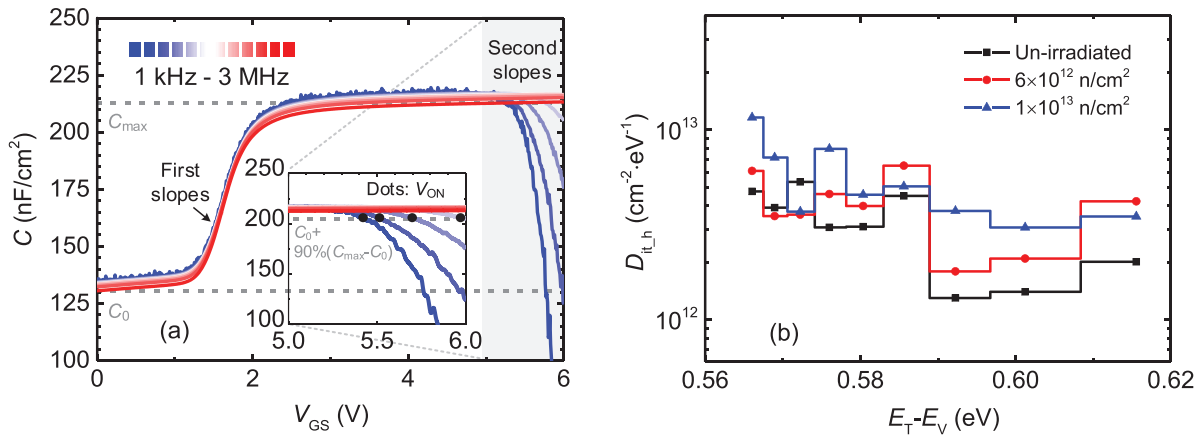


FIG. 2. (a) Measured C - V curves of P-GaN gate stack in GaN devices irradiated at the fluence of $1 \times 10^{14} \text{ n/cm}^2$ with a frequency from 1 kHz to 3 MHz; inset shows the enlarged view of second slopes showing V_{ON} defined at $C = C_0 + 90\%(C_{max} - C_0)$; (b) extracted hole traps density $D_{it,h}$ vs energy level of GaN devices including un-irradiated and irradiated at fluences of 6×10^{13} and $1 \times 10^{14} \text{ n/cm}^2$, respectively.

traps at the P-GaN/AlGaIn interface when massive holes are injected from the gate at high V_G .¹⁸ The traps density can be determined using the relationship between shifts of onset voltage V_{ON} of the second slopes and frequency, where V_{ON} is defined as the V_{GS} when C reaches 90% of the difference between maximum C_{max} and zero-bias C_0 . The capacitor of the Schottky P-GaN gate stack can be modeled as the in-series connection of metal/P-GaN Schottky junction capacitor (C_{P-GaN}) and AlGaIn barrier layer capacitor (C_B), which is based on the assumption of full depletion of the P-GaN layer when its effective doping concentration is less than $1 \times 10^{18} \text{ cm}^{-3}$ and $V_{GS} > V_{TH}$.¹⁹ The hole traps density $D_{it,h}$ can be determined by²⁰

$$D_{it,h} = \frac{C_{P-GaN} \cdot \Delta V_{ON}}{q(E_{f1} - E_{f2})} - \frac{C_{P-GaN} + C_B}{q^2}, \quad (1)$$

where ΔV_{ON} is the difference between V_{ON} at the frequency of f_1 and f_2 ($f_1 < f_2$). The E_f is $\ln(v_t \sigma_p N_V / f) \cdot kT$, where v_t and σ_p are the thermal velocity and capture cross section of holes, respectively, and N_V is the effective density of states in the valence band. The energy level of hole traps is at $E_V + (E_{f1} + E_{f2})/2$.

Figure 2(b) shows the distribution of hole traps at the P-GaN/AlGaIn interface obtained according to (1) and the C - V curves of devices including un-irradiated and irradiated at fluences of 6×10^{13} and $1 \times 10^{14} \text{ n/cm}^2$, respectively. The extracted traps with a density $D_{it,h}$ of $\sim 10^{12} \text{ cm}^{-2} \cdot \text{eV}^{-1}$ at $E_V + 0.56 \text{ eV}$ to $E_V + 0.62 \text{ eV}$ can be corresponding to the complex of Ga_i with other native defects including $(3+/+)$ transition level of nitrogen vacancy.^{13,21} The Ga_i has a low migration barrier of 0.9 eV and could migrate toward and accumulate at the P-GaN/AlGaIn interface under the gate electric field.^{16,22} Due to the low activation energy of Ga_i and its interaction with V_{Ga} decorated dislocations (V_{Ga} -DL), numbers of hole traps formed by Ga_i are required to first passivate V_{Ga} -DLs.²³ Higher fluences of neutron irradiation introduce higher $D_{it,h}$ in the same order of $10^{12} \text{ cm}^{-2} \cdot \text{eV}^{-1}$ as shown in Fig. 2(b).

In order to examine the electron traps introduced by neutron irradiation in the P-GaN gate stack, pulse I - V measurement is carried out as shown in the inset of Fig. 3(a). In each period of t_p , traps are

filled by stress voltage V_{stress} in stress time t_{stress} then partially de-trapped in measurement time t_m , and V_{TH} is measured at the end.²⁴ The V_{stress} ranges from -4 to 6 V , and t_m is from $1 \mu\text{s}$ to 10 ms . The total pulse period t_p is 100 ms , so the traps with a longer emission time constant than t_m will remain filled with electrons, resulting in ΔV_{TH} . The electron traps density $D_{it,e}$ can be determined by

$$D_{it,e} = \frac{\epsilon_{P-GaN} \Delta V_{TH}}{q t_{P-GaN} (E_{f1} - E_{f2})}, \quad (2)$$

where ϵ_{P-GaN} and t_{P-GaN} are the dielectric constant and thickness of the P-GaN layer, respectively. The f is equivalent to $1/t_m$, and E_f is the same as that in C - V measurement but using the thermal velocity and capture cross section of electrons. The energy level of electron traps is at $E_C - (E_{f1} + E_{f2})/2$.

Figure 3(a) shows the ΔV_{TH} vs V_{stress} of -4 to 6 V with t_m of $1 \mu\text{s}$. The obvious positive ΔV_{TH} after V_{stress} of 0 to 5 V is due to the trapping of electrons, which are partially de-trapped in t_m . The ΔV_{TH} is reduced when V_{stress} is 5 to 6 V due to hole injection, which hinders the investigation of electron traps. Thus, the optimized V_{stress} of 4 V is used in Fig. 3(b) when t_m is swept from $1 \mu\text{s}$ to 10 ms . The positive ΔV_{TH} is reduced with higher t_m because more trapped electrons at deeper energy levels are de-trapped. Neutron irradiation with higher fluences induces more positive ΔV_{TH} and electron traps. The electron traps distribution extracted from Fig. 3(b) is shown in Fig. 3(c) with $D_{it,e}$ of 10^{11} - $10^{12} \text{ cm}^{-2} \cdot \text{eV}^{-1}$ at $E_C - 0.38 \text{ eV}$ to $E_C - 0.55 \text{ eV}$, which are corresponding to the complexes of V_{Ga} and native defects.²²

The physical mechanism behind the degradation of Schottky P-GaN/AlGaIn/GaN heterostructure gate stack after neutron irradiation can be addressed with the help of Fig. 4. Three interactions are dominating after neutron irradiation in the Mg-doped P-GaN layer, as illustrated in Fig. 4(a): (1) Ga atoms are scattered from the lattice sites to interstitial sites forming Ga_i and leaving V_{Ga} ; (2) Ga_i passivates the V_{Ga} decorated dislocation (V_{Ga} -DL) to be pure DL,²³ and (3) V_{Ga} is ionized to be negatively charged V_{Ga}^{3-} . Figure 4(b) shows the band diagram of the P-GaN/AlGaIn/GaN gate stack with $V_{GS} > 0$ after neutron irradiation. The gate-metal/P-GaN Schottky junction is reversely

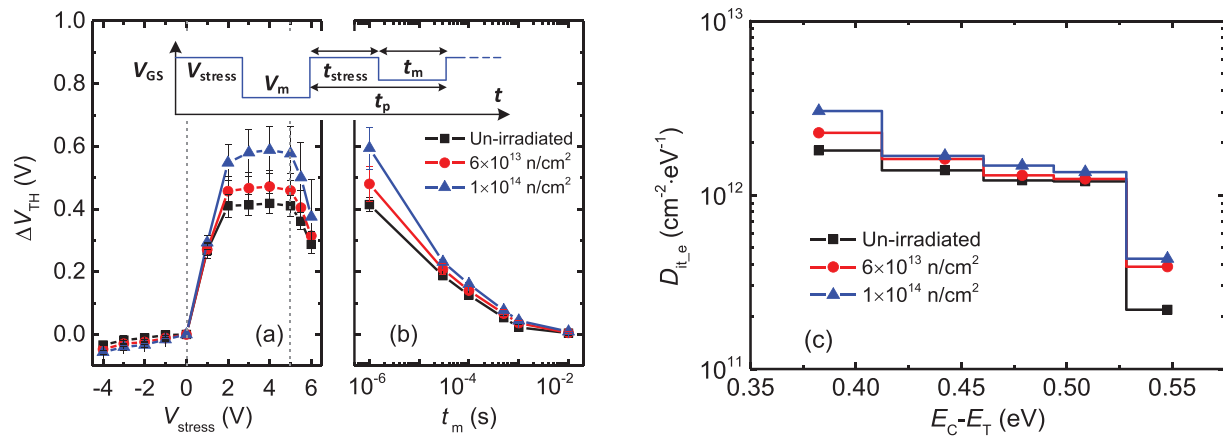


FIG. 3. (a) Measured ΔV_{TH} vs V_{stress} varying from -4 to 6 V, (b) ΔV_{TH} vs t_m varying from 1 μ s to 10 ms, and (c) extracted electron traps density $D_{it,e}$ vs energy level of GaN devices including un-irradiated and irradiated at fluences of 6×10^{13} and 1×10^{14} n/cm², respectively. The inset in (a) is the schematic setup of waveforms in pulse I-V measurement.

biased, and the depletion region is formed. The V_{Ga} induced by neutron irradiation will be ionized and trap electrons in the P-GaN layer, which eventually leads to positive shifts in V_{TH} .^{21,25} The Ga_i will first passivate the V_{Ga} -DLs, and the excessive Ga_i will be ionized when massive holes are injected from the gate when $V_{GS} > 5$ V, which leads to reduced positive ΔV_{TH} , as shown in Fig. 3(a).

From the first-principles calculation of the electronic states of dislocations, the states of pure DL are deeper than V_{Ga} -DL for the defects states above E_V .²⁶ The transmutation of V_{Ga} -DL to pure-DL modulates the energy band and leads to lower barrier height for holes, which is the same as the $q\Delta\phi_B$ of -0.017 and -0.031 eV extracted by Frenkel-Poole emission model after neutron irradiation at fluences of 6×10^{13} and 1×10^{14} n/cm², respectively. Meanwhile, the traps assisted tunneling at the metal/P-GaN interface is enhanced by the introduction of more traps in the depletion region of the P-GaN layer. Thus, the leakage current in the P-GaN/AlGaIn/GaN gate stack exhibits significant increases after neutron irradiation with higher fluences, as shown in Fig. 1(c).

Based on the proposed mechanism for degradation, two kinds of measures can be taken to make the GaN power devices with Schottky

P-GaN stack more resistant to neutron radiation: reducing the density of inherent traps and increasing the height of potential barriers in the heterostructure. First, in order to counter the introduction of traps by neutron irradiation, the quality P-GaN/AlGaIn/GaN heterostructure needs to be improved. The density of thread dislocations and point defects should be further reduced both in body and at interface of the heterostructure. Second, in order to reduce the trapping and de-trapping of carriers in the gate stack, the height of potential barriers in the heterostructure needs to be increased. The gate leakage current, which consists of injected carriers over the barriers, should be reduced. Practical measures include adding reinforcement layers such as thin GaON or Al₂O₃ layers at surface or interface,²⁷ adding n-type GaN on P-GaN to form metal/N-GaN/P-GaN/AlGaIn/GaN heterostructure,²⁸ and using metals with a high work function as the gate material.²⁹

In conclusion, the mechanism of degradation of Schottky P-GaN gate stack in GaN power devices under neutron irradiation is investigated. After neutron irradiation at fluences of 6×10^{13} and 1×10^{14} n/cm², the devices exhibit positive ΔV_{TH} and increased gate leakage current. The C-V and pulse I-V measurements have revealed the existence of electron traps at E_C - (0.38–0.55) eV and hole traps at

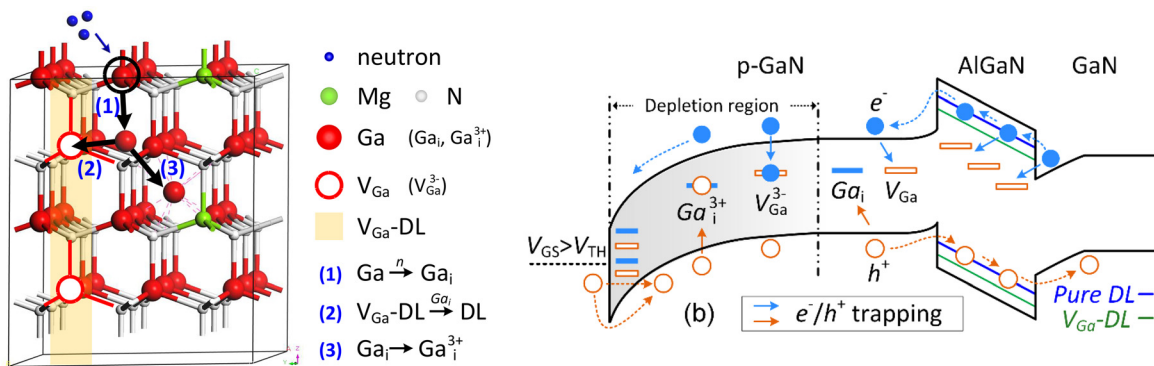


FIG. 4. (a) Schematic atomic structures showing the interactions between the V_{Ga} , Ga_i , and the V_{Ga} decorated dislocation (V_{Ga} -DL) in Mg-doped P-GaN and (b) band diagram of P-GaN/AlGaIn/GaN gate stack with $V_{GS} > V_{TH}$ after neutron irradiation.

$E_V + (0.56\text{--}0.62)$ eV with the density of $10^{11}\text{--}10^{12}\text{ cm}^{-2}\text{ eV}^{-1}$ after neutron irradiation. Higher positive ΔV_{TH} and larger gate leakage current are observed in devices under neutron irradiation with higher fluences due to the incremental introduction of traps. The ionizations of V_{Ga} and Ga_i induced by neutron irradiation as well as their interactions with dislocations significantly alter the energy band of P-GaN/AlGaIn/GaN heterostructure. The trapping and de-trapping processes of electron traps lead to positive shifts in V_{TH} . Passivation of dislocations by Ga_i effectively lowers the barrier height for holes and leads to increased gate leakage current. This work depicts the physical process and mechanism of degradations in Schottky P-GaN gate stack under neutron irradiation, which can provide deeper insights into the analysis and field application of GaN power devices in the extreme environment with high fluences of neutron irradiation.

DATA AVAILABILITY

The data that support the findings of this study are available from the corresponding author upon reasonable request.

REFERENCES

- C. Zeitlin, D. M. Hassler, F. A. Cucinotta, B. Ehresmann, R. F. Wimmer-Schweingruber, D. E. Brinza, S. Kang, G. Weigle, S. Böttcher, E. Böhm, S. Burmeister, J. Guo, J. Köhler, C. Martin, A. Posner, S. Rafkin, and G. Reitz, *Science* **340**(6136), 1080 (2013).
- S. J. Pearton, A. Aitkaliyeva, M. Xian, F. Ren, A. Khachatrian, A. Ildefonso, Z. Islam, M. A. Jafar Rasel, A. Haque, and A. Y. Polyakov, *ECS J. Solid State Sci. Technol.* **10**(5), 055008 (2021).
- H. Y. Xiao, F. Gao, X. T. Zu, and W. J. Weber, *J. Appl. Phys.* **105**(12), 123527 (2009).
- S. J. Pearton, R. Deist, F. Ren, L. Liu, A. Y. Polyakov, and J. Kim, *J. Vac. Sci. Technol. A* **31**(5), 050801 (2013).
- E. Holmström, A. Kuronen, and K. Nordlund, *Phys. Rev. B* **78**(4), 045202 (2008).
- J. Autran and D. Munteanu, *IEEE Trans. Nucl. Sci.* **67**(7), 1428 (2020).
- A. Y. Polyakov, N. B. Smirnov, A. V. Govorkov, A. V. Markov, N. G. Kolin, D. I. Merkurisov, V. M. Boiko, K. D. Shcherbatchev, V. T. Bublik, M. I. Voronova, S. J. Pearton, A. Dabiran, and A. V. Osinsky, *J. Vac. Sci. Technol. B* **24**(5), 2256 (2006).
- P. A. Butler, M. J. Uren, B. Lambert, and M. Kuball, *IEEE Trans. Nucl. Sci.* **65**(12), 2862 (2018).
- A. Y. Polyakov, N. B. Smirnov, A. V. Govorkov, A. V. Markov, S. J. Pearton, N. G. Kolin, D. I. Merkurisov, and V. M. Boiko, *J. Appl. Phys.* **98**(3), 033529 (2005).
- F. Berthet, S. Petitdidier, Y. Guhel, J. L. Trolet, P. Mary, C. Gaquière, and B. Boudart, *IEEE Trans. Nucl. Sci.* **63**(3), 1918 (2016).
- J. C. Petrosky, J. W. McClory, T. E. Gray, and T. A. Uhlman, *IEEE Trans. Nucl. Sci.* **56**(5), 2905 (2009).
- K. Kuriyama, M. Ooi, A. Onoue, K. Kushida, M. Okada, and Q. Xu, *Appl. Phys. Lett.* **88**(13), 132109 (2006).
- Z. Zhang, A. R. Arehart, E. C. H. Kyle, J. Chen, E. X. Zhang, D. M. Fleetwood, R. D. Schrimpf, J. S. Speck, and S. A. Ringel, *Appl. Phys. Lett.* **106**(2), 022104 (2015).
- M. Ahmed, B. Kucukgok, A. Yanguas-Gil, J. Hryn, and S. A. Wender, *Radiat. Phys. Chem.* **166**, 108456 (2020).
- N. Xu, R. Hao, F. Chen, X. Zhang, H. Zhang, P. Zhang, X. Ding, L. Song, G. Yu, K. Cheng, Y. Cai, and B. Zhang, *Appl. Phys. Lett.* **113**(15), 152104 (2018).
- S. Limpijumngong and C. G. Van de Walle, *Phys. Rev. B* **69**(3), 035207 (2004).
- J. Xu, R. Wang, L. Zhang, S. Zhang, P. Zheng, Y. Zhang, Y. Song, and X. Tong, *Appl. Phys. Lett.* **117**(2), 023501 (2020).
- M. Tápajna, O. Hilt, E. Bahat-Treidel, J. Würfl, and J. Kuzmík, *Appl. Phys. Lett.* **107**(19), 193506 (2015).
- F. Wang, W. Chen, R. Sun, Z. Wang, Q. Zhou, and B. Zhang, *J. Phys. D: Appl. Phys.* **54**(9), 095107 (2021).
- N. Ramanan, L. Bongmook, and V. Misra, *Trans. Electron Devices* **62**(2), 546 (2015).
- S. Yang, S. Huang, J. Wei, Z. Zheng, Y. Wang, J. He, and K. J. Chen, *IEEE Electron Dev. Lett.* **41**(5), 685 (2020).
- J. Neugebauer and C. G. Van de Walle, *Phys. Rev. B* **50**(11), 8067 (1994).
- R. Wang, J. Xu, S. Zhang, Y. Zhang, P. Zheng, Z. Cheng, L. Zhang, F.-X. Chen, X. Tong, and Y. Zhang, *J. Mater. Chem. C* **9**(9), 3177 (2021).
- S. Yang, S. Liu, Y. Lu, C. Liu, and K. J. Chen, *IEEE Trans. Electron Devices* **62**(6), 1870 (2015).
- X. Li, B. Bakeroort, Z. Wu, N. Amirifar, S. You, N. Posthuma, M. Zhao, H. Liang, G. Groeseneken, and S. Decoutere, *IEEE Electron Device Lett.* **41**(4), 577 (2020).
- R. Wang, X. Tong, J. Xu, C. Dong, Z. Cheng, L. Zhang, S. Zhang, P. Zheng, F.-X. Chen, Y. Zhang, and W. Tan, *Phys. Rev. Appl.* **14**(2), 024039 (2020).
- L. Zhang, Z. Zheng, S. Yang, W. Song, S. Feng, and K. J. Chen, *Appl. Phys. Lett.* **119**(5), 053503 (2021).
- C. Wang, M. Hua, J. Chen, S. Yang, Z. Zheng, J. Wei, L. Zhang, and K. J. Chen, *IEEE Electron Device Lett.* **41**(4), 545 (2020).
- F. Lee, L. Su, C. Wang, Y. Wu, and J. Huang, *IEEE Electron Device Lett.* **36**(3), 232 (2015).